Supplementary Information

Effect of Cyano group in Colour-tunability of Aryl-substituted Buta-1,3-Diene based Solid-state Emissive Copolymers

Prasanta Pal,[a] Ayan Datta, [a] Susmita Mukherjee,[b] Ajay Perumal[*b] and Sudip Malik [a*]

[a] School of Applied & Interdisciplinary Sciences (SAIS), Indian Association for the Cultivation of Science, 2A and 2B Raja S. C. Mullick Road, Jadavpur, Kolkata-700032, E-mail: psusm2@iacs.res.in

[b] Functional NANO and Opto-electronics Lab (FNOL), Department of Physical Sciences, Indian Institute of Science Education and Research (IISER), Berhampur, Odisha, India-760010, E-mail ajay@iiserbpr.ac.in

Table of Content: **Page No.**

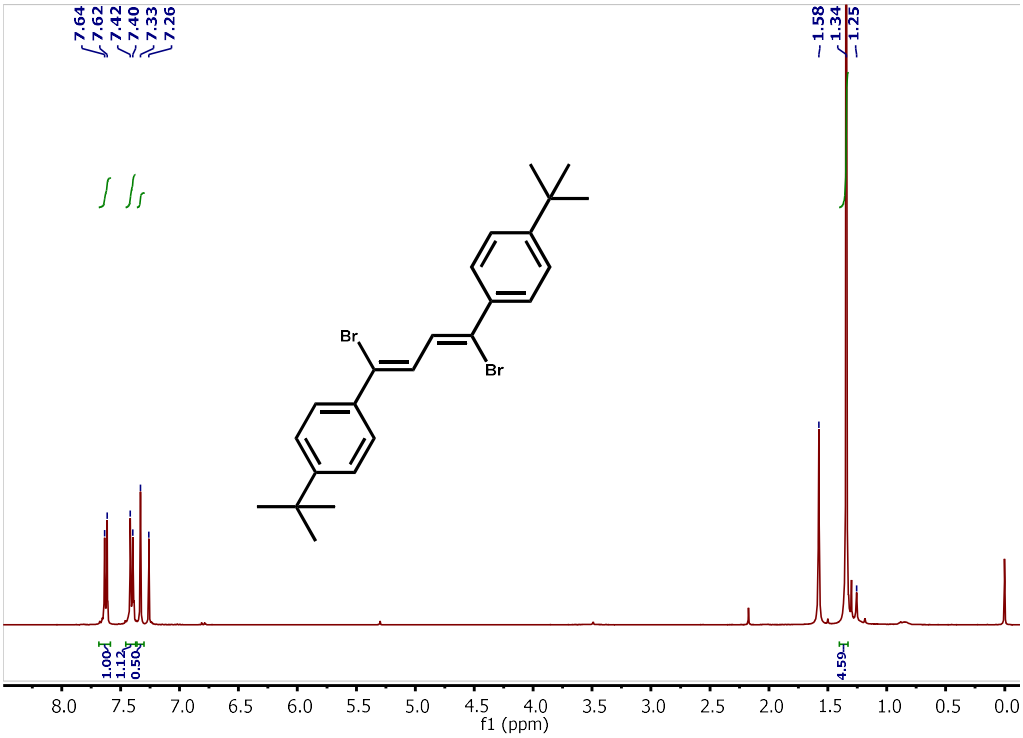

Fig.S1: ^{1}H NMR of (1Z, 3Z)-1, 4-dibromo-1,4-ditertbutylphenyl-buta-1,3-diene (1)

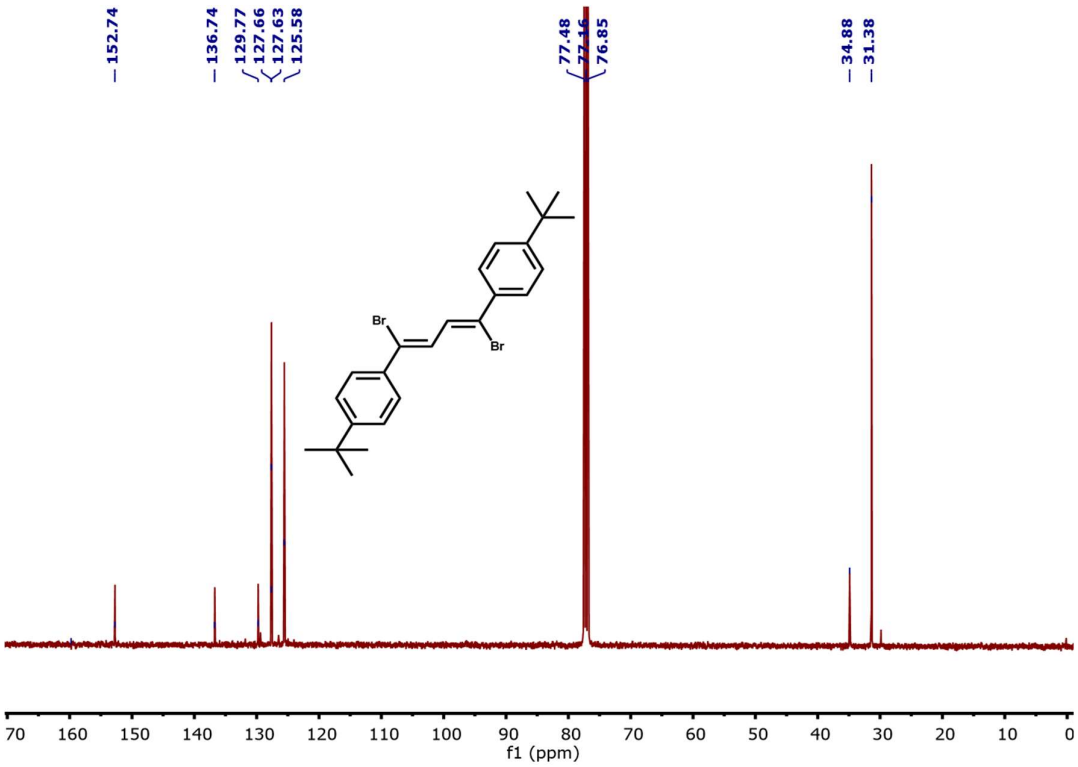

Fig.S2: ^{13}C NMR of (1Z, 3Z)-1, 4-dibromo-1,4-ditertbutylphenyl-buta-1,3-diene (1)

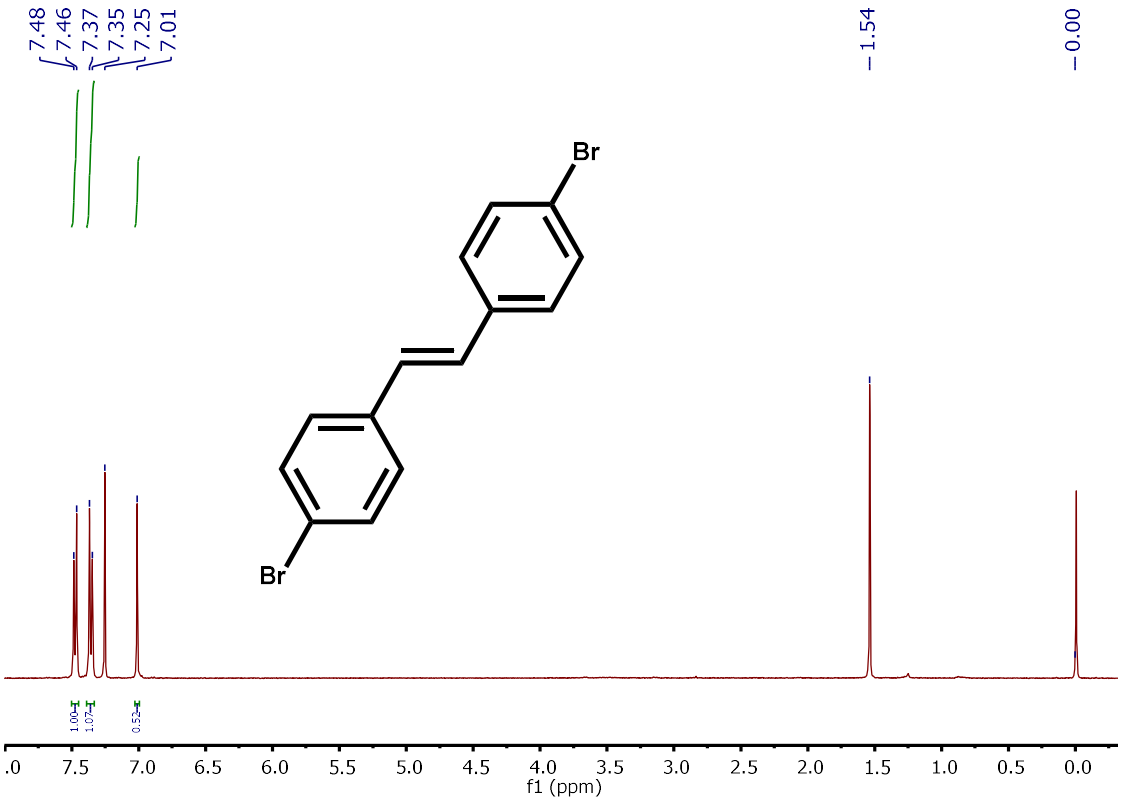

Fig.S3: ^{1}H NMR of (E)-1,2-Bis(4-bromophenyl)ethene (2)

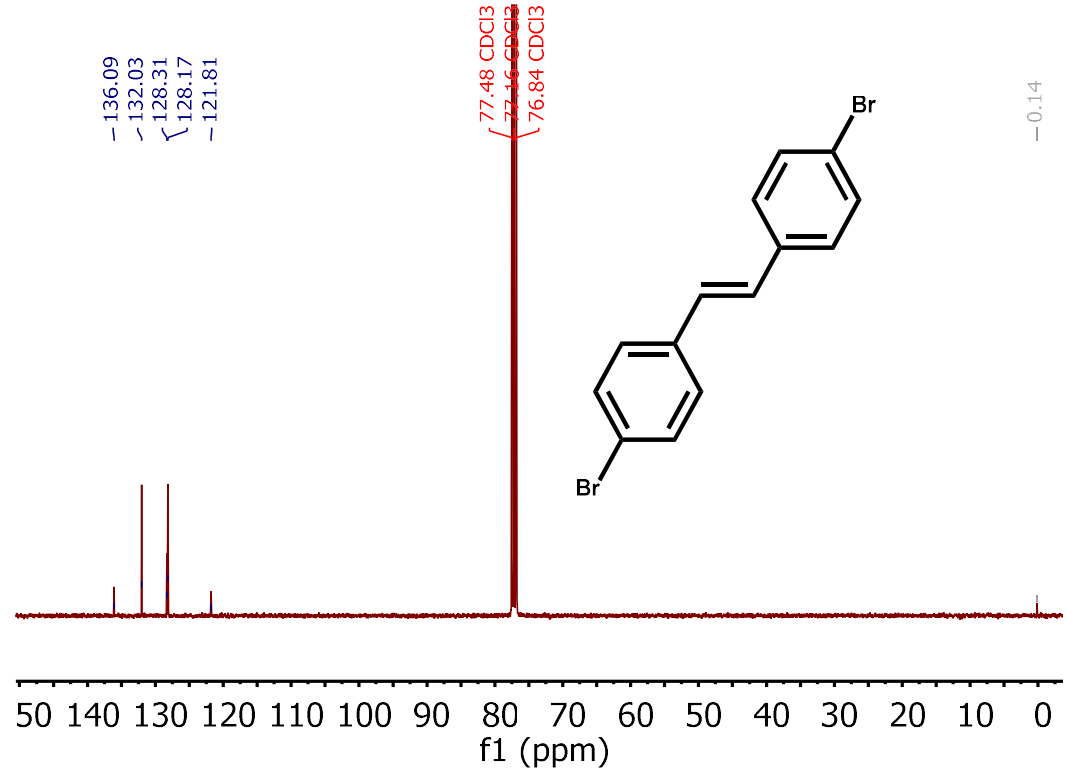

Fig.S4: ^{13}C NMR of (E)-1,2-Bis(4-bromophenyl)ethene (2)

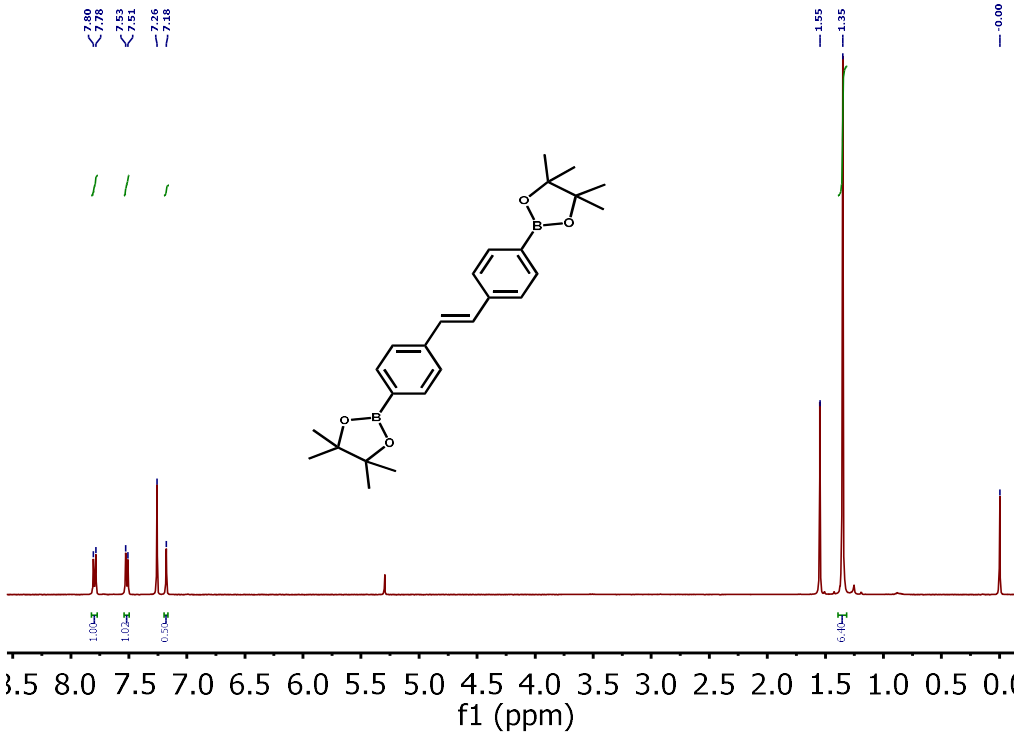

Fig.S5: ^{1}H NMR of (E)-1,2-Bis(4-(4,4,5,5-tetramethyl-1,3,2-dioxaborolan-2-yl)-phenyl)ethene (5)

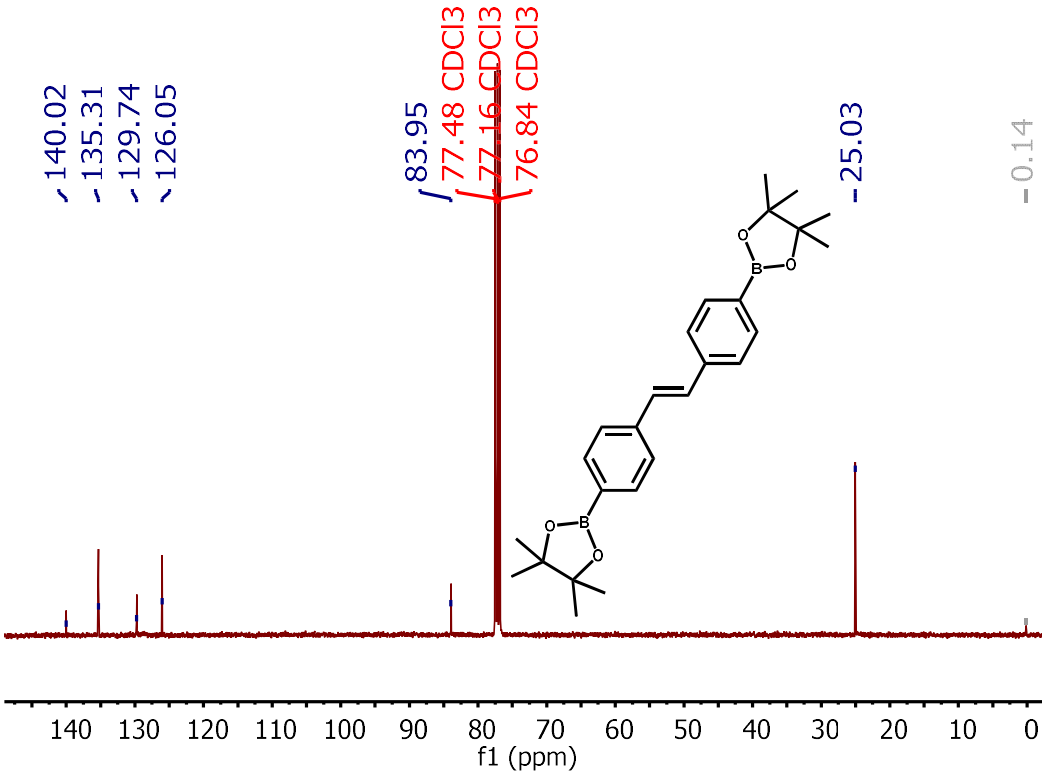

Fig. S6: ^{13}C NMR of (E)-1,2-Bis(4-(4,4,5,5-tetramethyl-1,3,2-dioxaborolan-2-yl)-phenyl)ethene (5)

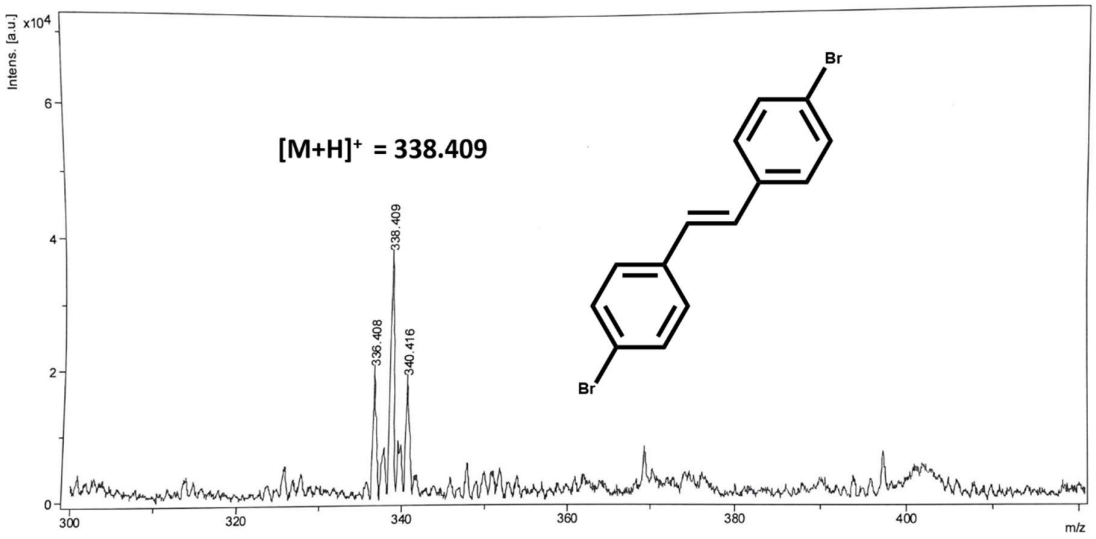

Fig.S7: MALDI-TOF mass of (E)-1,2-Bis(4-bromophenyl)ethene (2)

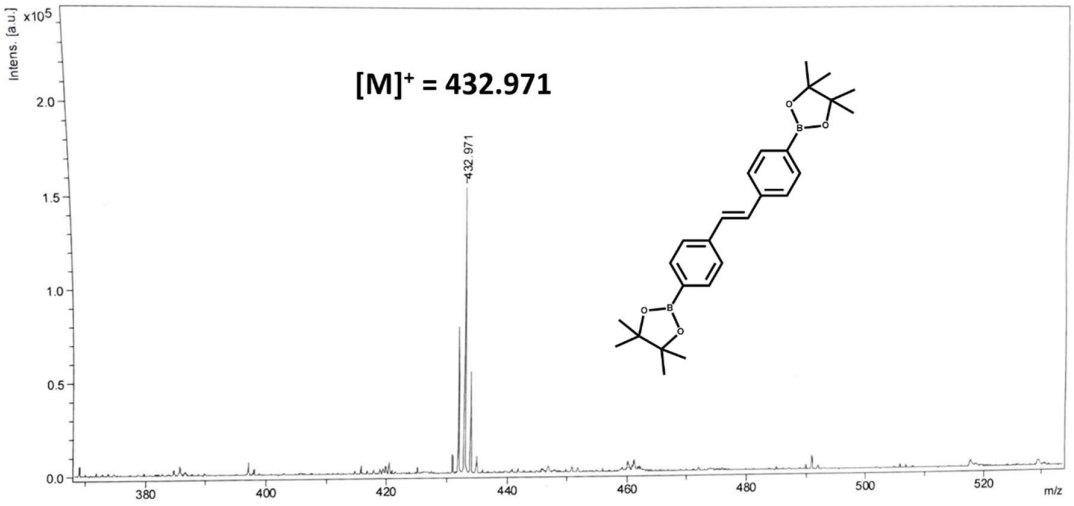

Fig.S8: MALDI-TOF mass of (E)-1,2-Bis(4-(4,4,5,5-tetramethyl-1,3,2-dioxaborolan-2-yl)-phenyl)ethene (5)

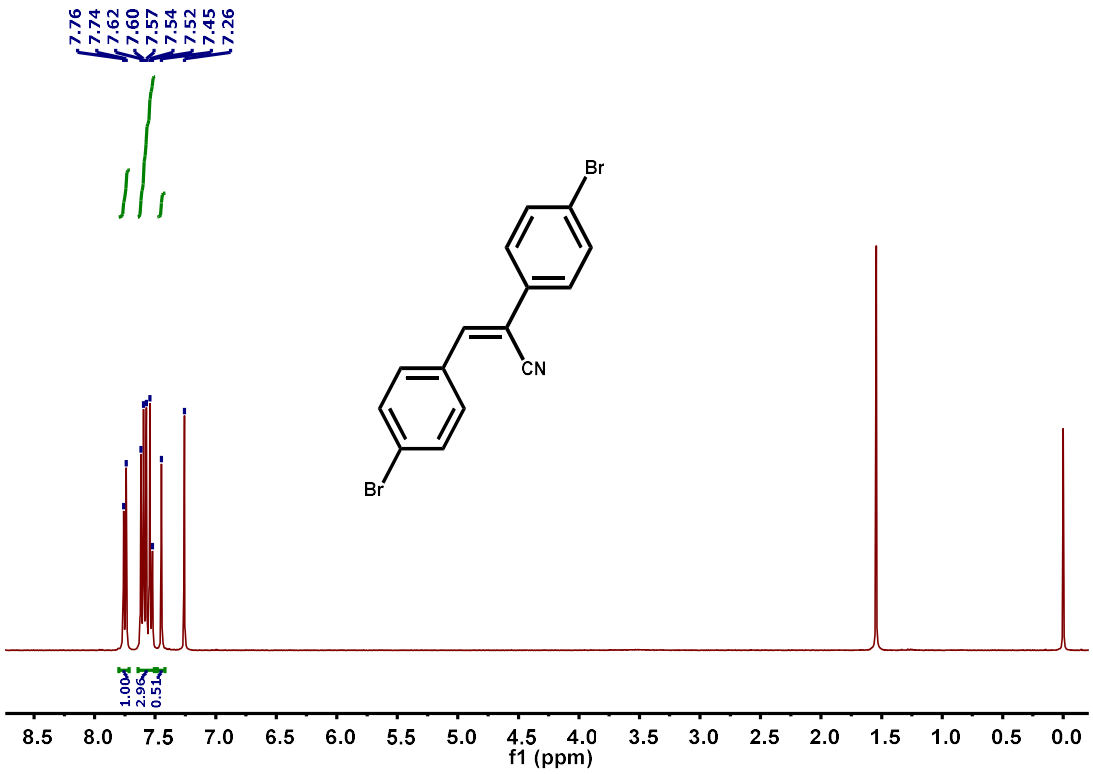

Fig.S9: ^{1}H NMR of (Z)-2,3-bis(4-bromophenyl)acrylonitrile (3)

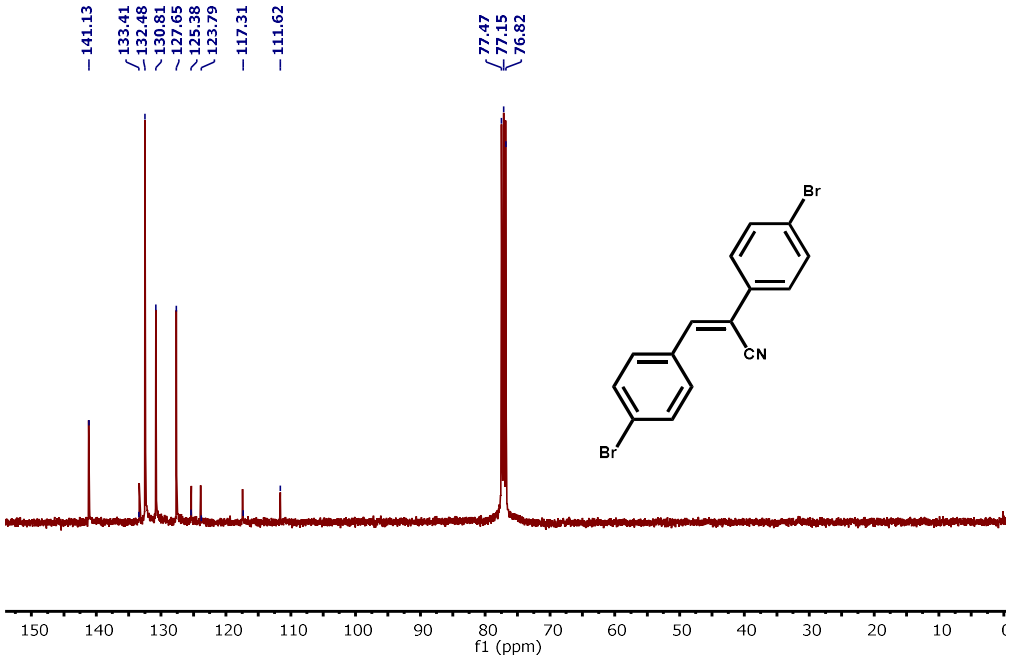

Fig.S10: ^{13}C NMR of (Z)-2,3-bis(4-bromophenyl)acrylonitrile (3)

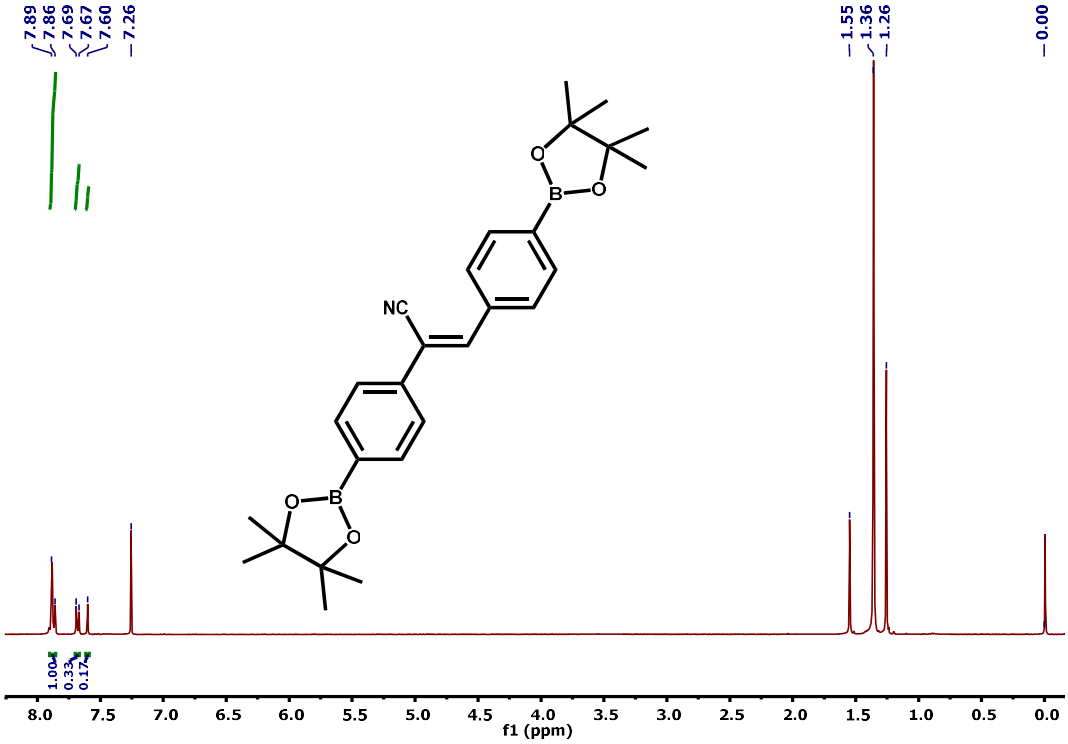

Fig.S11: ^{1}H NMR of (Z)-2,3-bis(4-(4,4,5,5-tetramethyl-1,3,2-dioxaborolan-yl)phenyl)acrylonitrile(6)

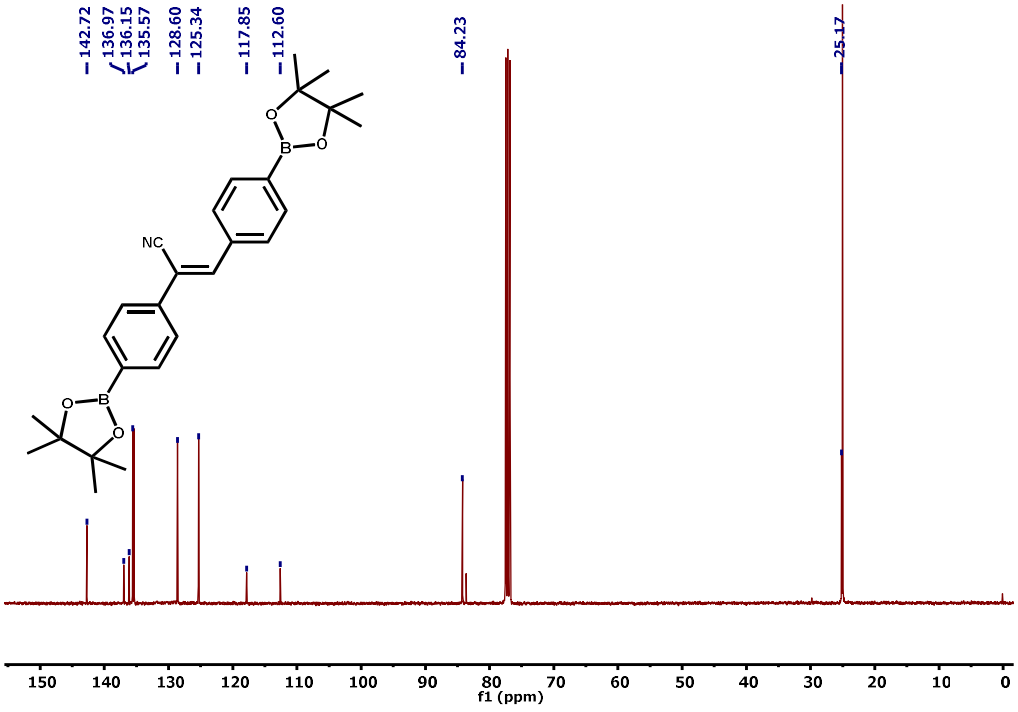

Fig.S12: ^{13}C NMR of (Z)-2,3-bis(4-(4,4,5,5-tetramethyl-1,3,2-dioxaborolan-yl)phenyl)acrylonitrile(6)

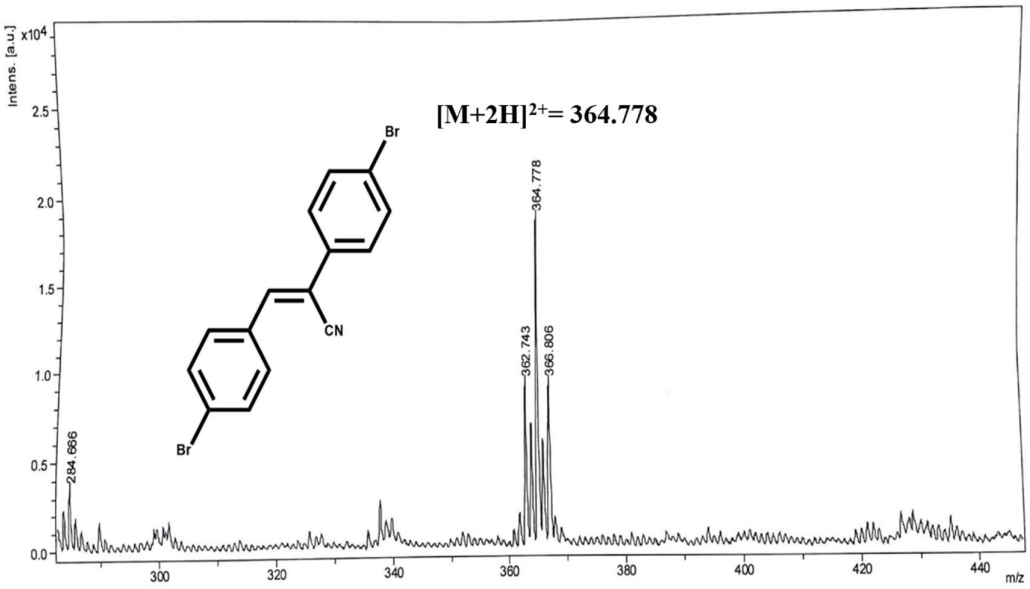

Fig.S13: MALDI-TOF mass of (Z)-2,3-bis(4-bromophenyl)acrylonitrile (3)

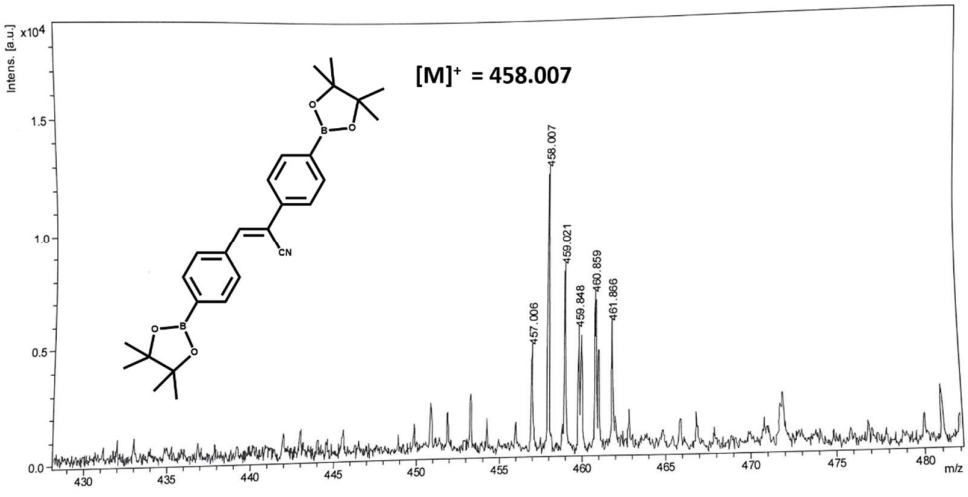

Fig.S14: MALDI-TOF mass of (Z)-2,3-bis(4-(4,4,5,5-tetramethyl-1,3,2-dioxaborolan-yl)phenyl)acrylonitrile(6)

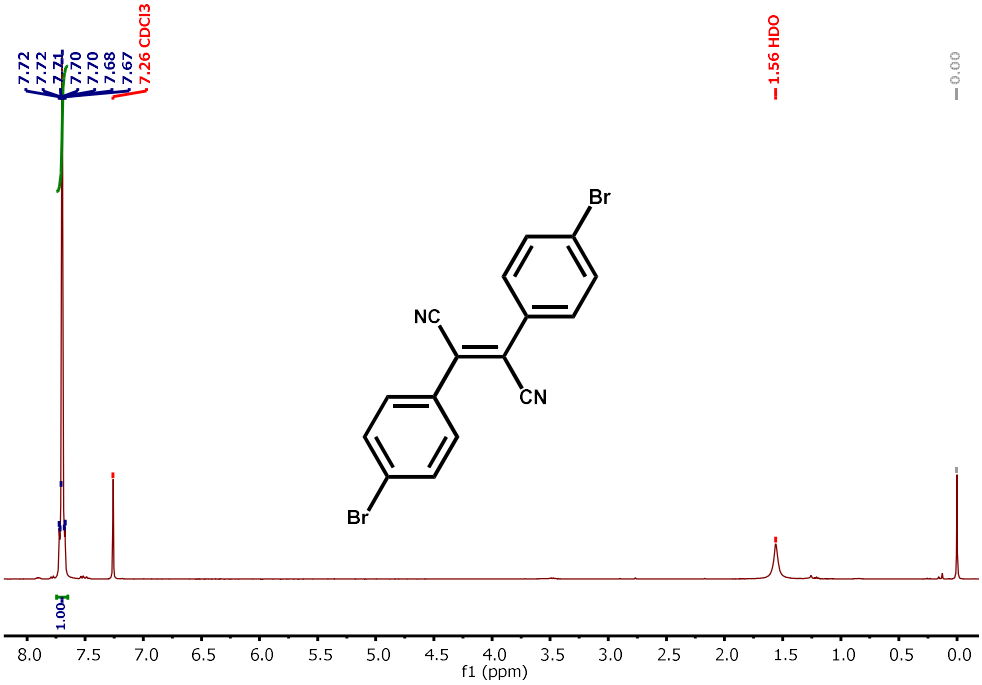

Fig.S15: ^{1}H NMR of 3-bis(4-bromophenyl) fumaronitrile(4)

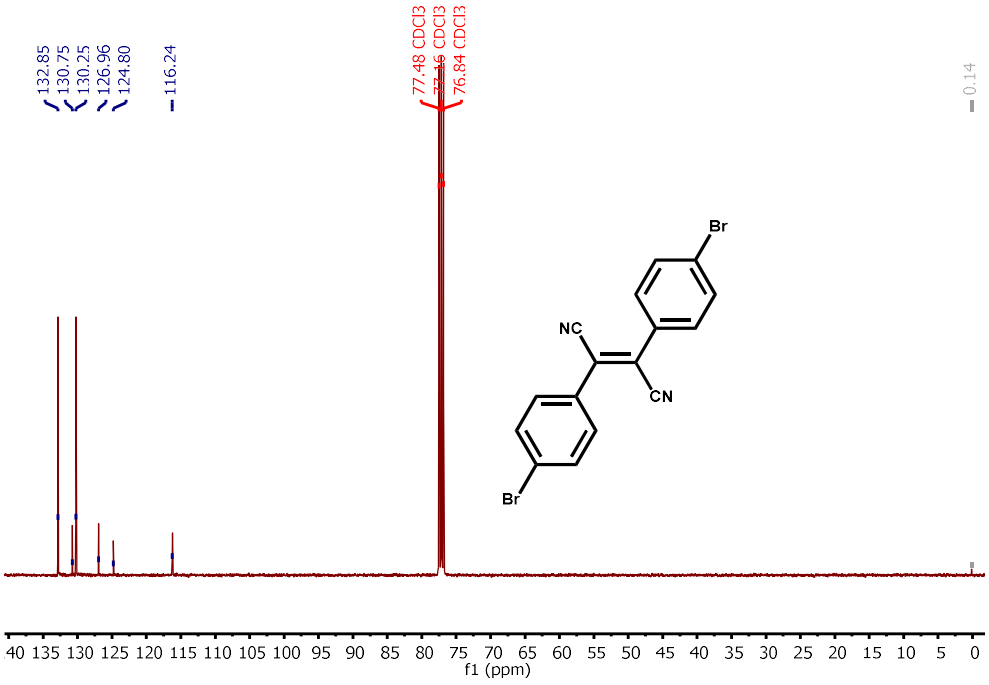

Fig.S16: ^{13}C NMR of 2,3-bis(4-bromophenyl) fumaronitrile(4)

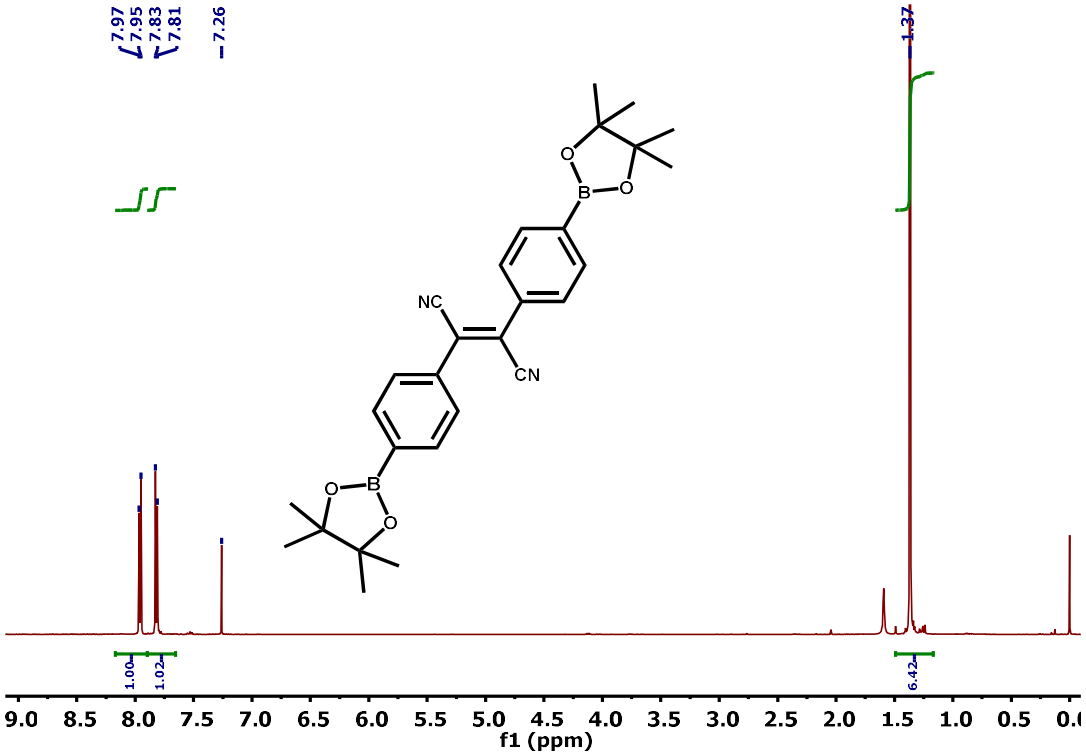

Fig.S17: ^{1}H NMR of 2,3-bis(4-(4,4,5,5-tetramethyl-1,3,2-dioxaborolanyl)phenyl)-fumaronitrile(7)

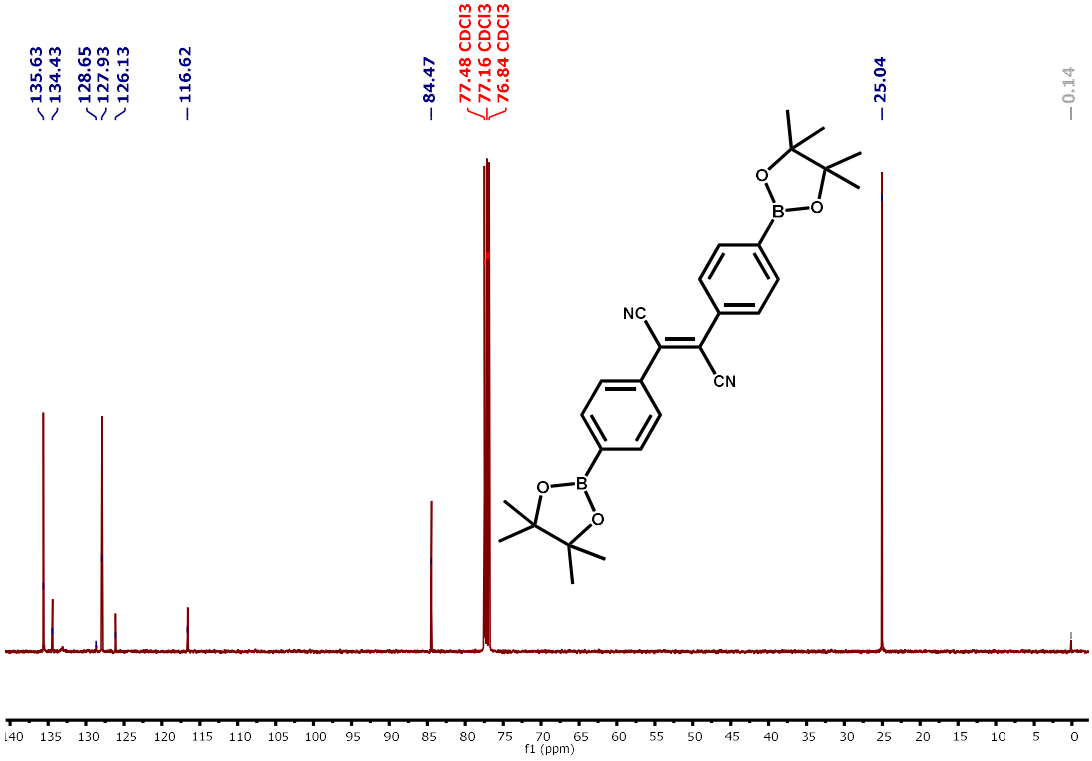

Fig.S18: ^{13}C NMR of 2,3-bis(4-(4,4,5,5-tetramethyl-1,3,2- dioxaborolanyl)phenyl)-fumaronitrile(7).

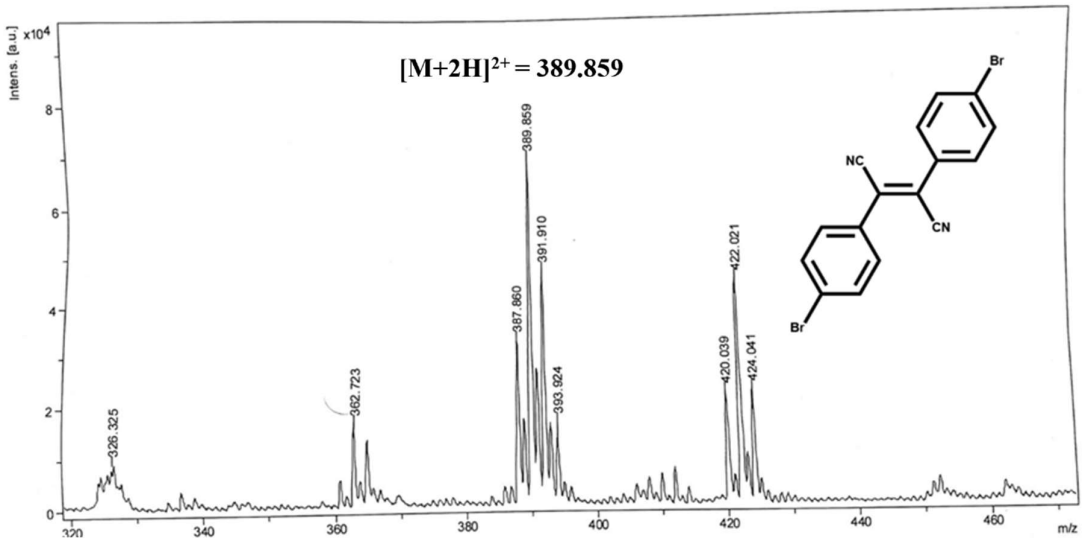

Fig. S19: MALDI-TOF mass of 2,3-bis(4-bromophenyl)fumaronitrile(4)

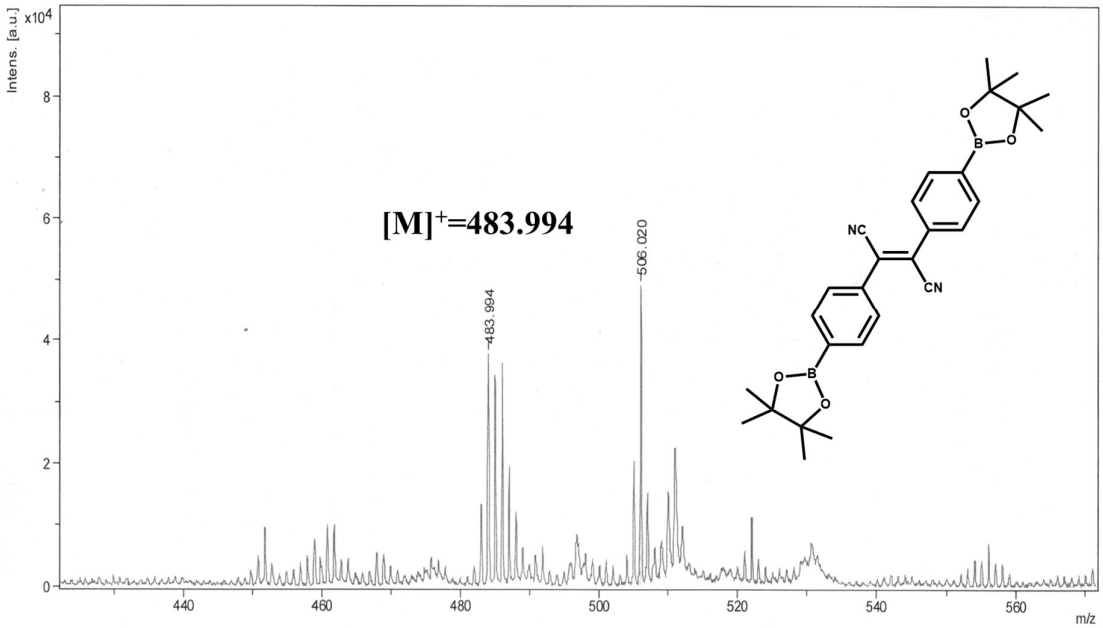

Fig. S20: MALDI-TOF mass of 2,3-bis(4-(4,4,5,5-tetramethyl-1,3,2-dioxaborolanyl)phenyl)fumaronitrile (7)

(a)

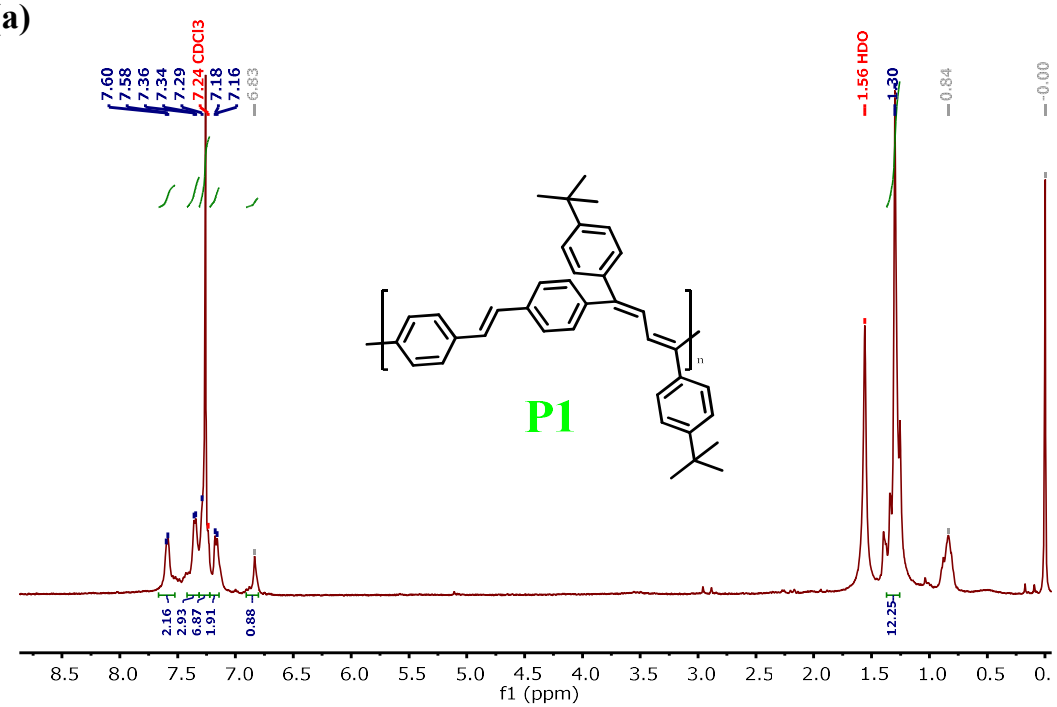

(b)

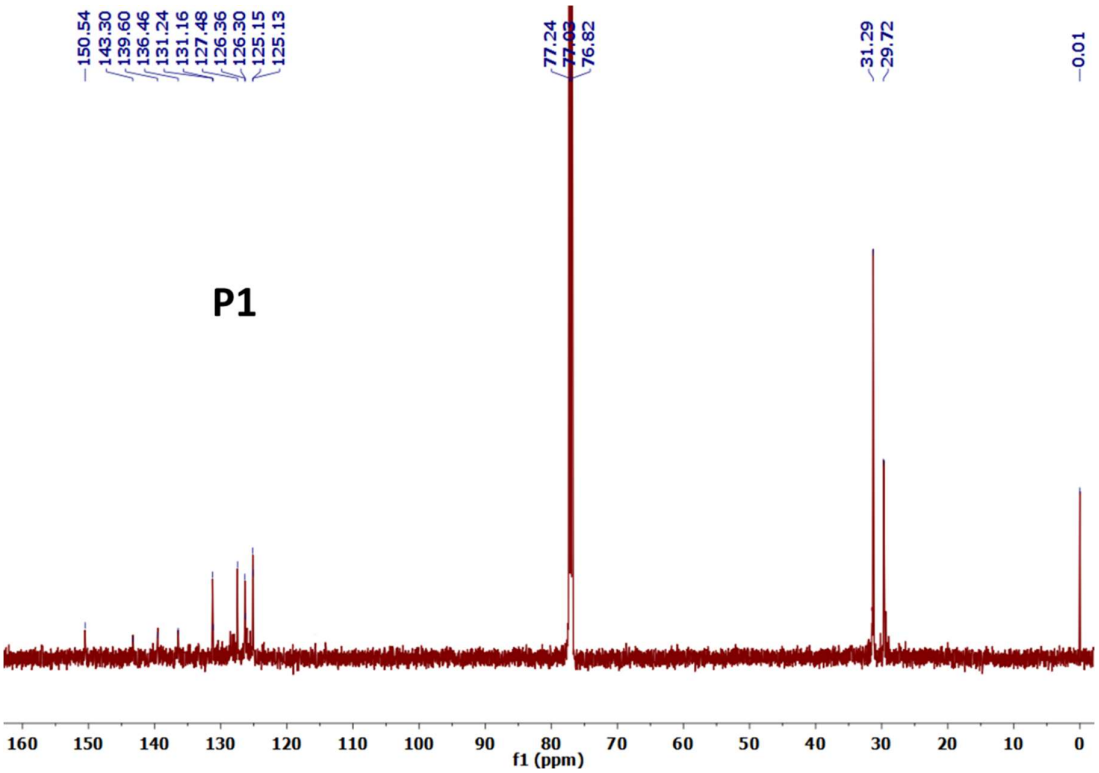

Fig. S21: (a) ^{1}H NMR and (b) ^{13}C NMR of copolymer, P1 in $CDCl_3$.

(a)

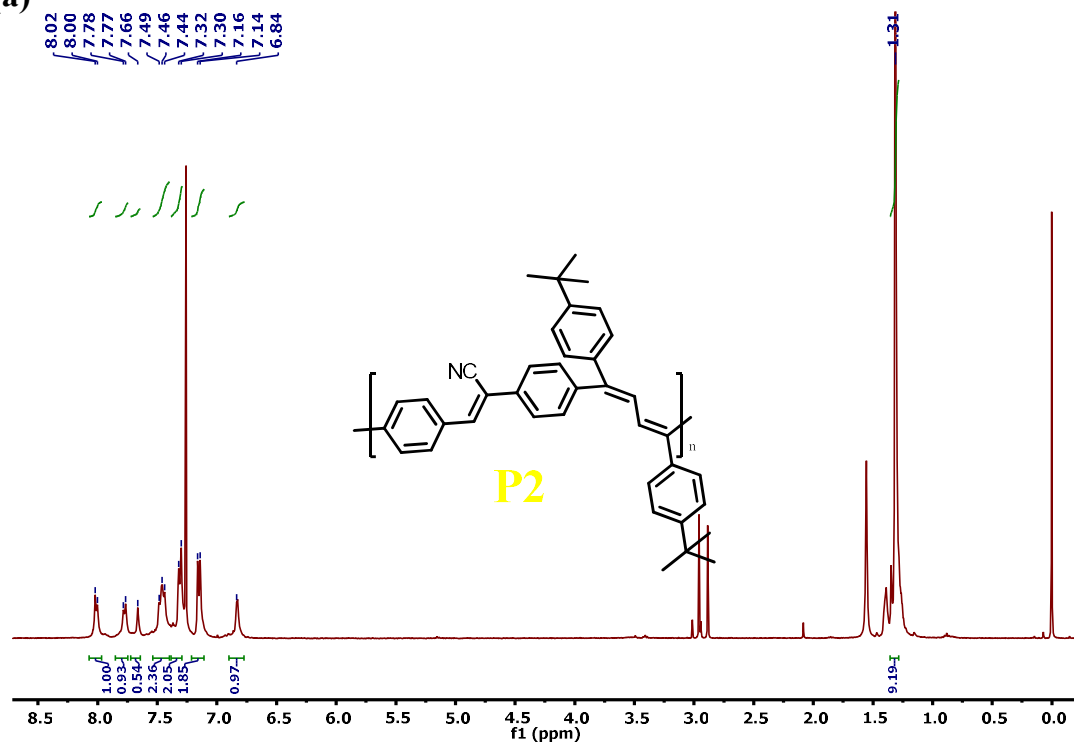

(b)

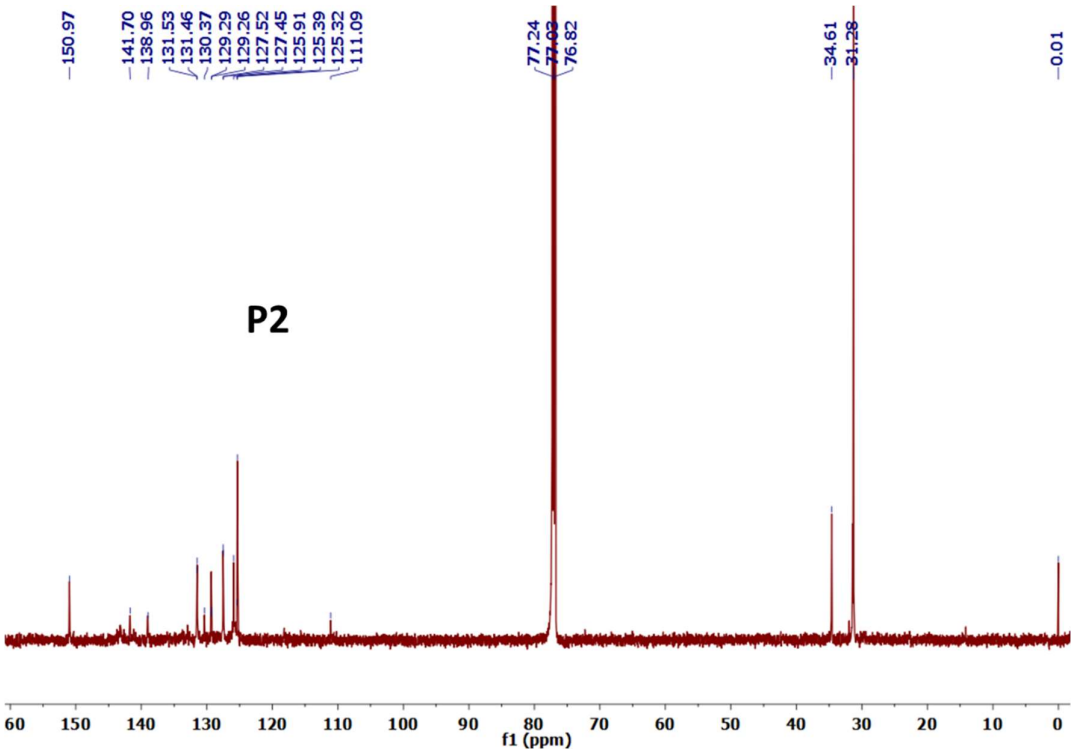

Fig. S22: (a) ^{1}H NMR and (b) ^{13}C NMR of copolymer, P2 in $CDCl_3$.

(a)

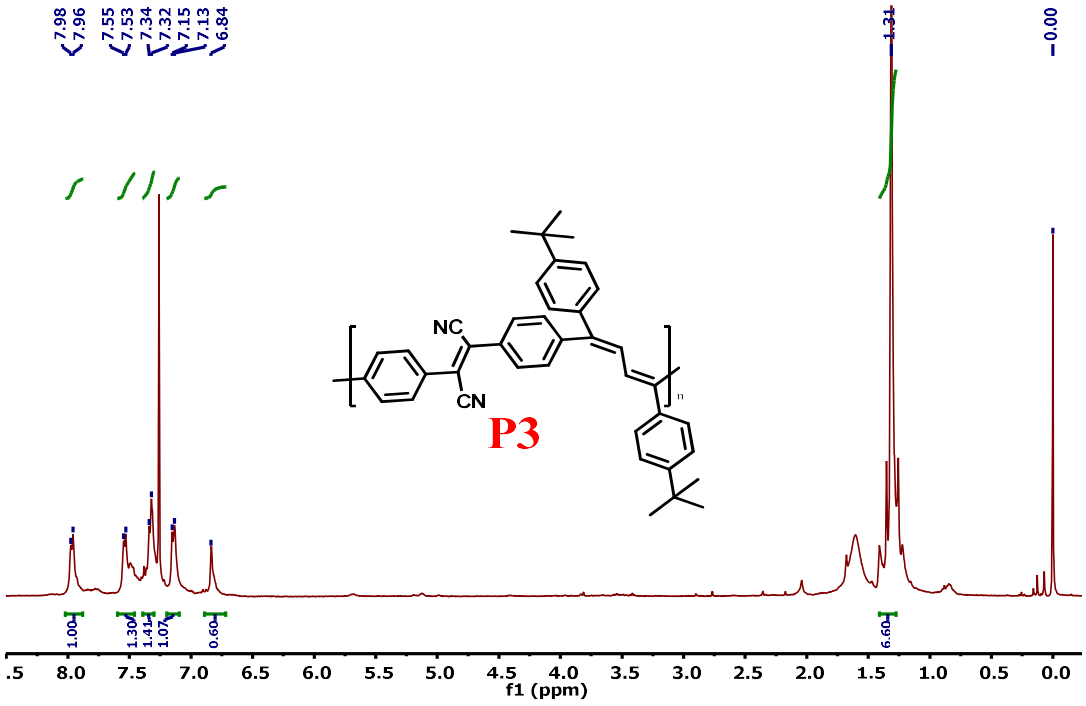

(b)

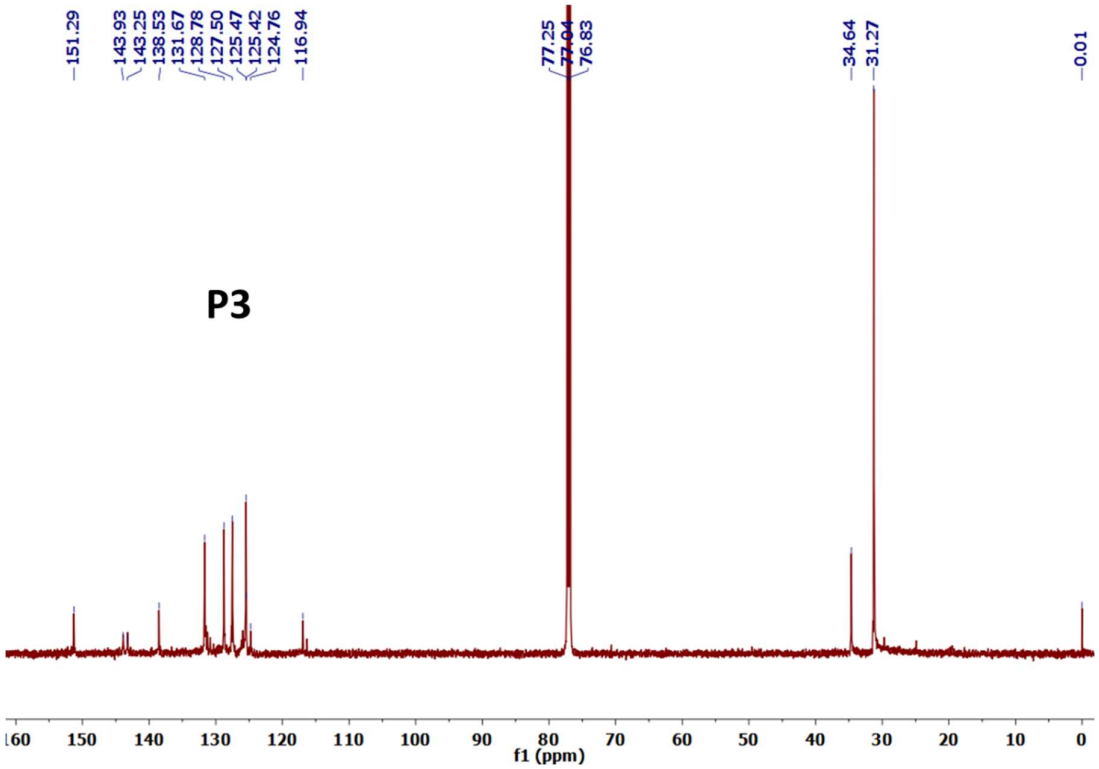

Fig. S23: (a) ^{1}H NMR and (b) ^{13}C NMR of copolymer, P3 in $CDCl_3$.

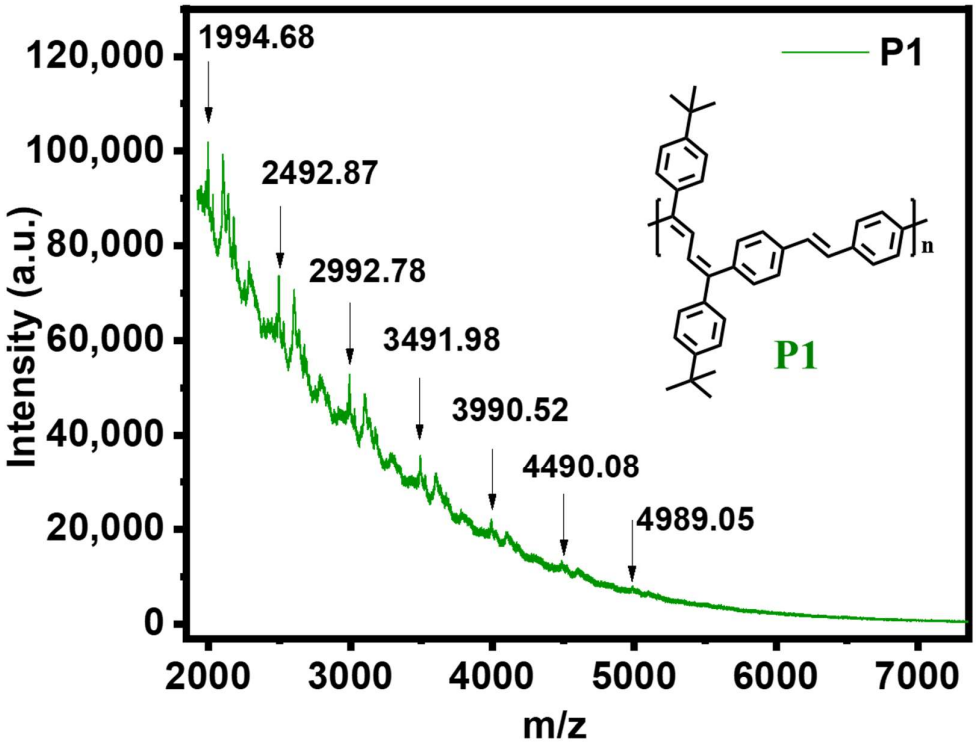

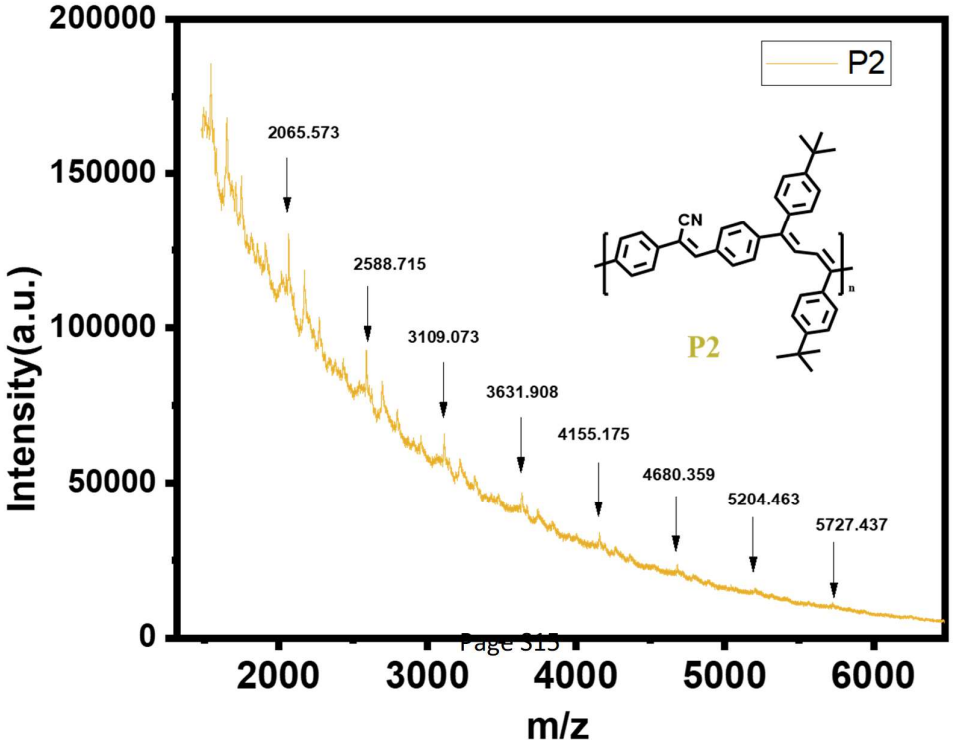

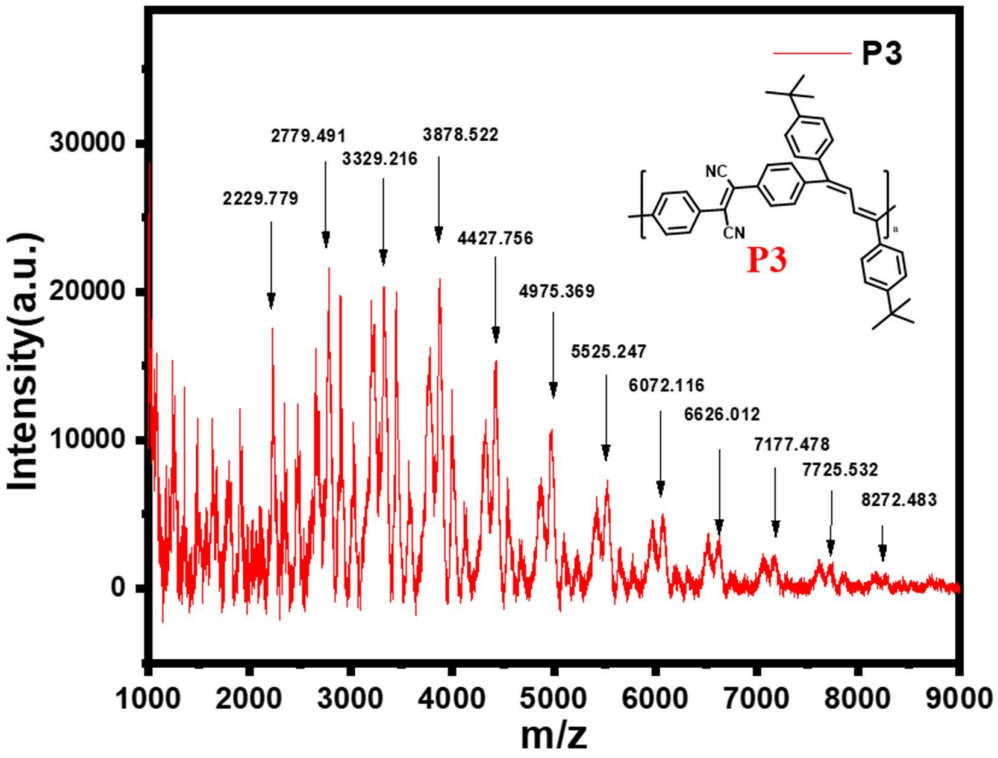

Fig. S24: MALDI-TOF spectra of copolymers, P1, P2 and P3 in dithranol matrix.

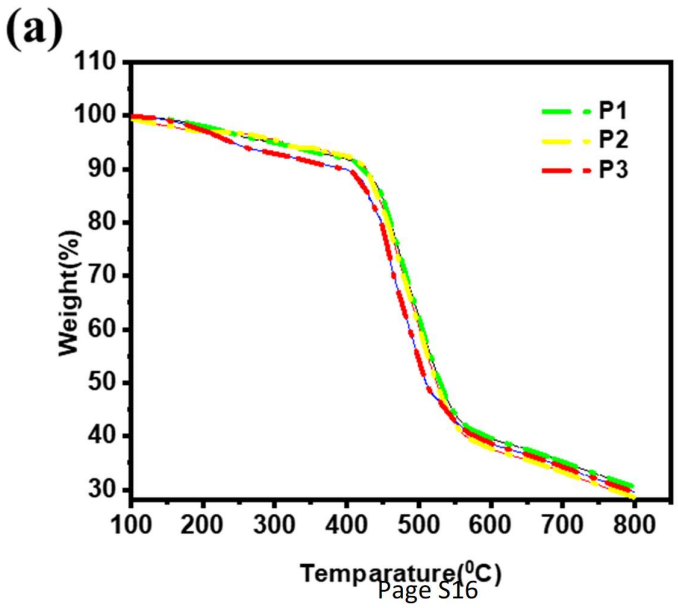

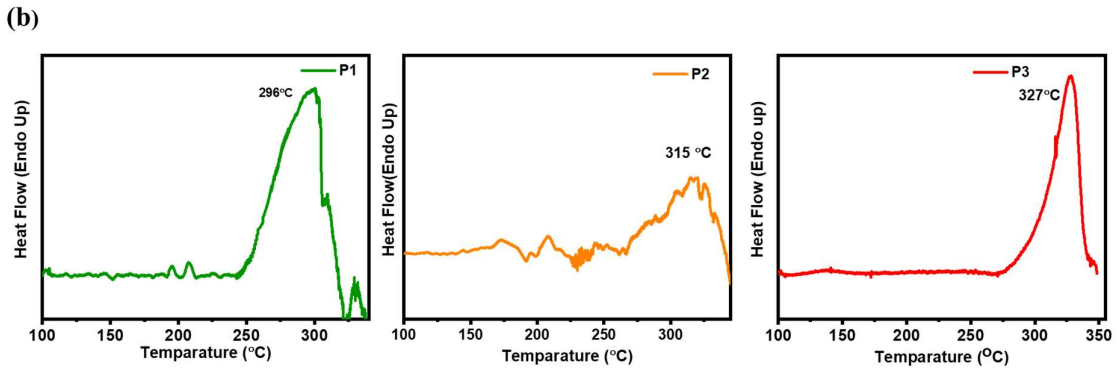

Fig. S25: (a) TGA traces of copolymers P1, P2 and P3 and (b) DSC trace of copolymer P1, P2 and P3 (the phase transition peak at 296 °C, 315 °C and 327 °C and the enthalpy change 1.6 J/g, 3.5 J/g and 8.1 J/g respectively)

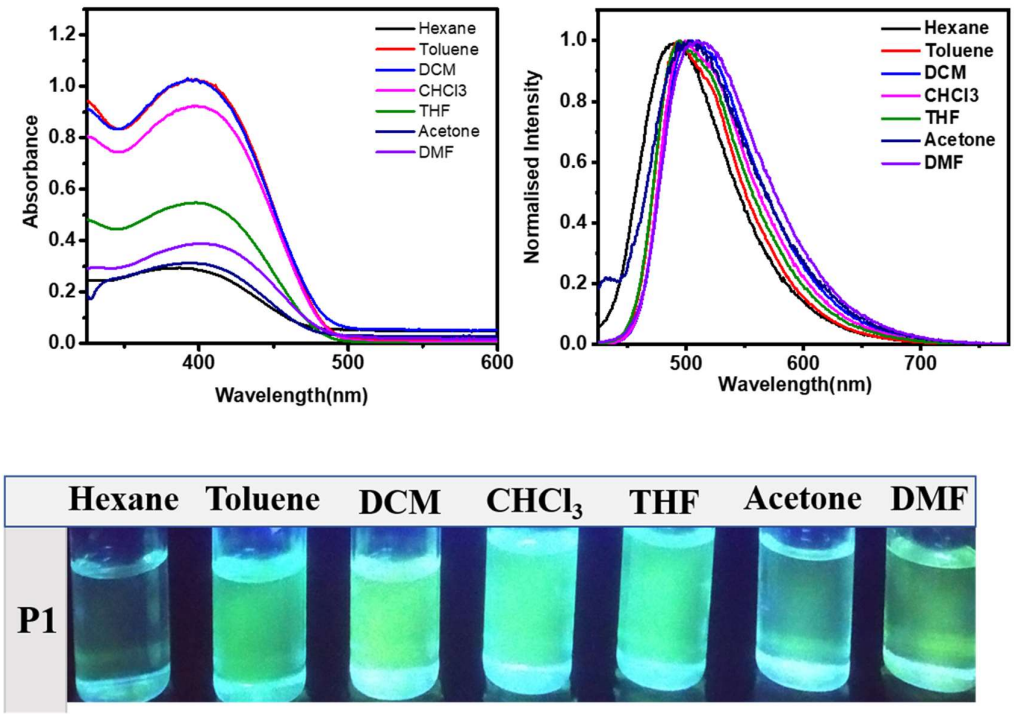

Fig. S26: Solvent dependent UV-Vis and fluorescence spectra (upper) and fluorescence color in various solvents under UV light (lower) of copolymer, P1.

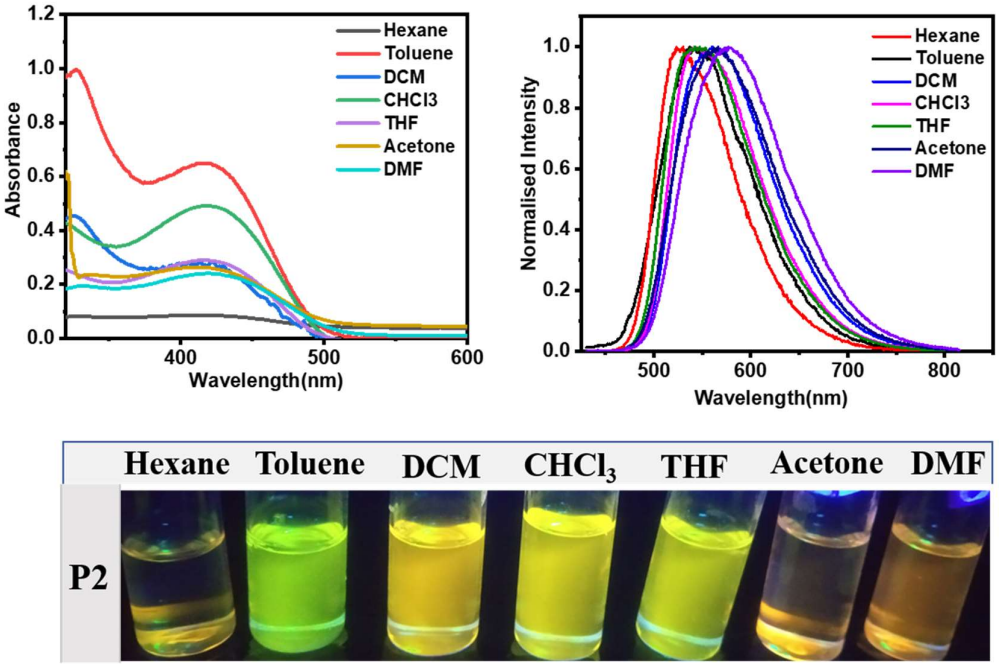

Fig. S27: Solvent dependent UV-Vis and fluorescence spectra (upper) and fluorescence color in various solvents under UV light (lower) of copolymer, P2.

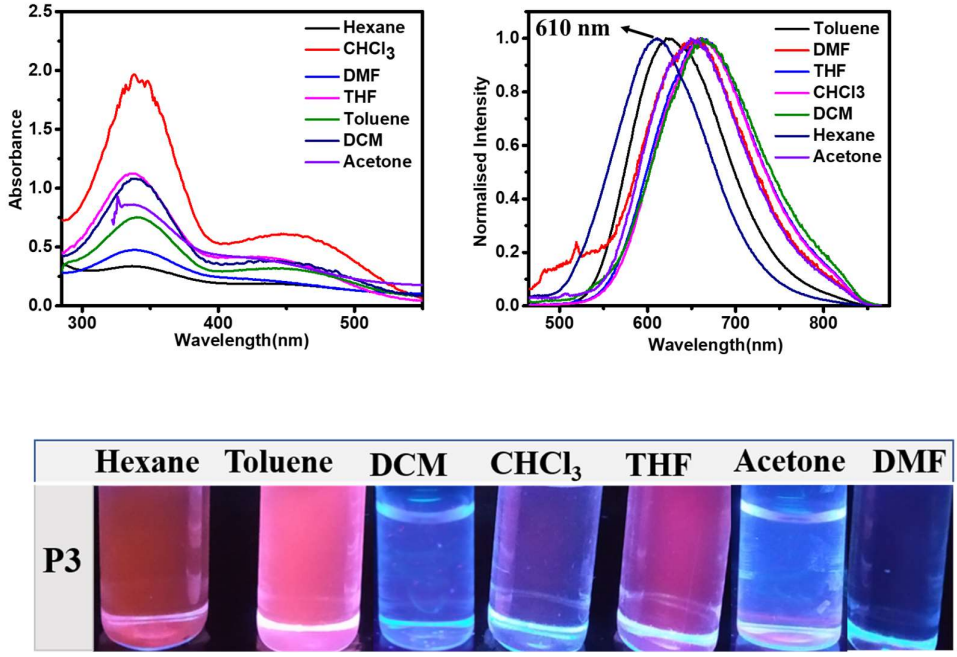

Fig. S28: Solvent dependent UV and fluorescence spectra (upper) and fluorescence color in various solvents under UV light (lower) of copolymer, P3.

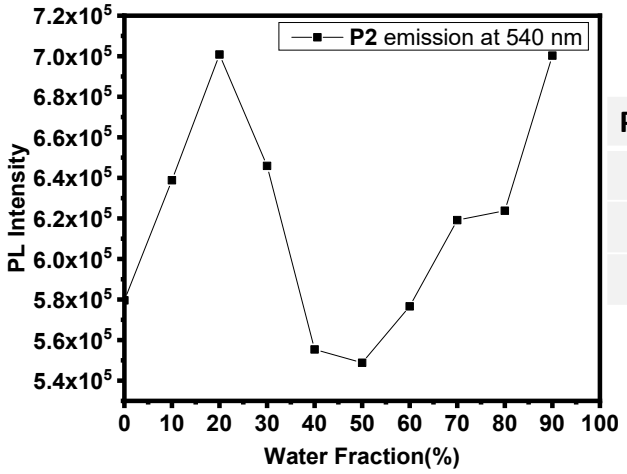

Polymer	Solution	Film
P1	0.28, 0.53	0.36, 0.58
P2	0.45, 0.53	0.51, 0.48
P3	0.61, 0.38	0.66, 0.34

Fig. S29: Emission intensity change vs water fraction (%) of copolymer, P2 and CIE coordinates calculated from CIE chromaticity diagram.

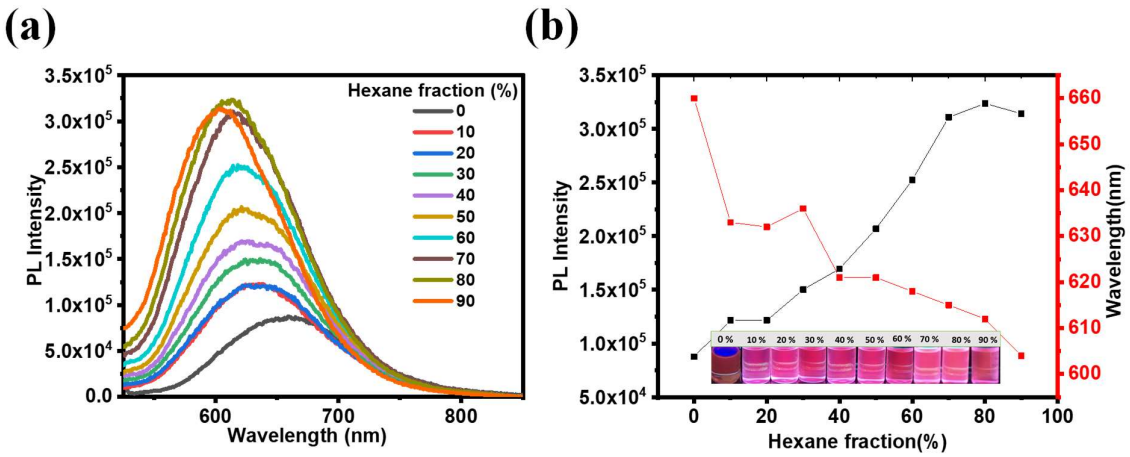

Fig. S30: (a) Emission spectra of P3 in hexane/THF mixture (b) Plot of emission intensity/wavelength vs hexane fraction (%), emission colour at different hexane fraction (inset) of copolymer, P3.

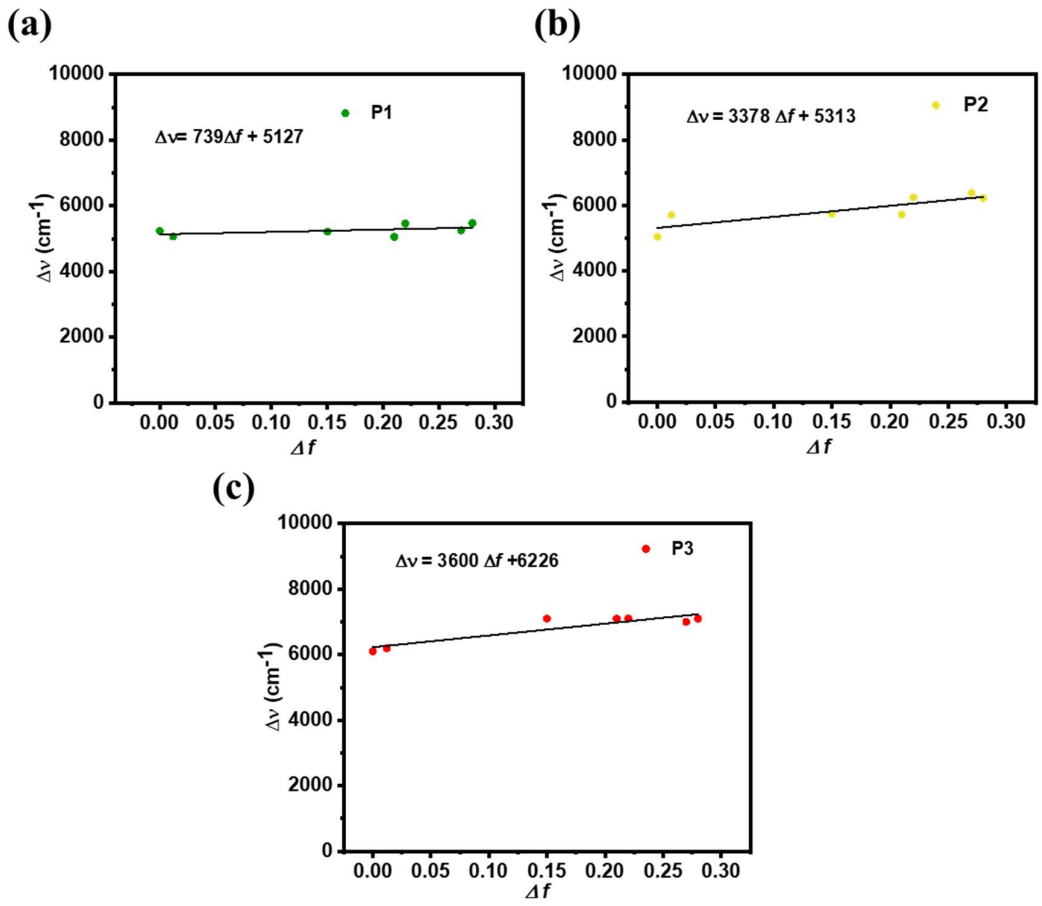

Fig. S31: Lippert-Mataga plot with best liner fitting of the copolymers for (a) P1 (b) P2 and (c) P3. Values were taken from Table-S1.

To better understand the effects of solvatochromic, the relationship between the solvent polarity parameter (Δf) and the Stokes shift ($\Delta\upsilon$, cm^{-1}) according to the Lippert–Mataga equation was investigated according to reported equation.

Table -S1: Value for Lippert-Mataga plot [S1]

Copolymer	Solvent	Δf	λ_{abs} (nm)	λ_{FL} (nm)	Stokes shift ($\Delta\upsilon$, cm^{-1})
P1	Hexane	0.00	390	490	5232
	Toluene	0.01	395	494	5073
	DCM	0.22	394	502	5460
	$CHCl_3$	0.15	396	499	5213
	THF	0.21	398	498	5045
	Acetone	0.28	395	504	5475
	DMF	0.27	399	505	5252
P2	Hexane	0.00	417	528	5041
	Toluene	0.01	415	544	5714
	DCM	0.22	416	562	6244
	$CHCl_3$	0.15	418	550	5741
	THF	0.21	416	546	5723
	Acetone	0.28	418	565	6224
	DMF	0.27	418	570	6379
P3	Hexane	0.00	445	611	6105
	Toluene	0.01	450	624	6197
	DCM	0.22	450	664	7162
	$CHCl_3$	0.15	450	662	7116
	THF	0.21	450	660	7070
	Acetone	0.28	445	651	7110
	DMF	0.27	445	650	7087

Copolymer	Slope value	Intercept value	Correlation coefficient (R^2)
P1	739	5127	0.27
P2	3378	5313	0.71
P3	3600	6226	0.83

Table-S2: TCSPC data of copolymers.

Compound	α_1	α_2	α_3	τ_1(ns)	τ_2(ns)	τ_3(ns)	χ^2	<τ> ns
P1 solution	47.41	34.62	17.97	0.227077	0.074506	0.66	**1.19**	**0.42**
P1 film	32.31	54.76	12.93	0.360455	0.107237	1.23733	**1.09**	**0.74**
P2 solution	63.00	37.00	----	0.400747	0.862562	-----	**1.17**	**0.66**
P2 film	64.64	35.36	----	0.342494	1.10716	------	**1.15**	**0.83**
P3 solution	39.88	60.12	----	0.281633	0.822291	-----	**1.12**	**0.73**
P3 film	28.01	71.99	----	0.6247	2.30879	----	**1.19**	**2.14**

Fluorescence lifetimes were measured through Time-Correlated Single Photon Counting (TCSPC) with Horiba Jobin Yvon Fluoromax 3 spectrometer with magic angle with 405 nm and 450 nm laser probe. The decay curves were fitted with biexponential for **P2** and **P3** solution and film state and P1 in triexponential. The spectra were taken in DCM and spin coated on quartz glass for film state. The average fluorescence lifetimes were measured using the equation-

Average fluorescence lifetime, **<τ>** = $\sum_i \alpha_i \tau_i^2 \Big/ \sum_i \alpha_i \tau_i$

, Where 'α' is amplitude percentage and 'τ' is fluorescence lifetimes.

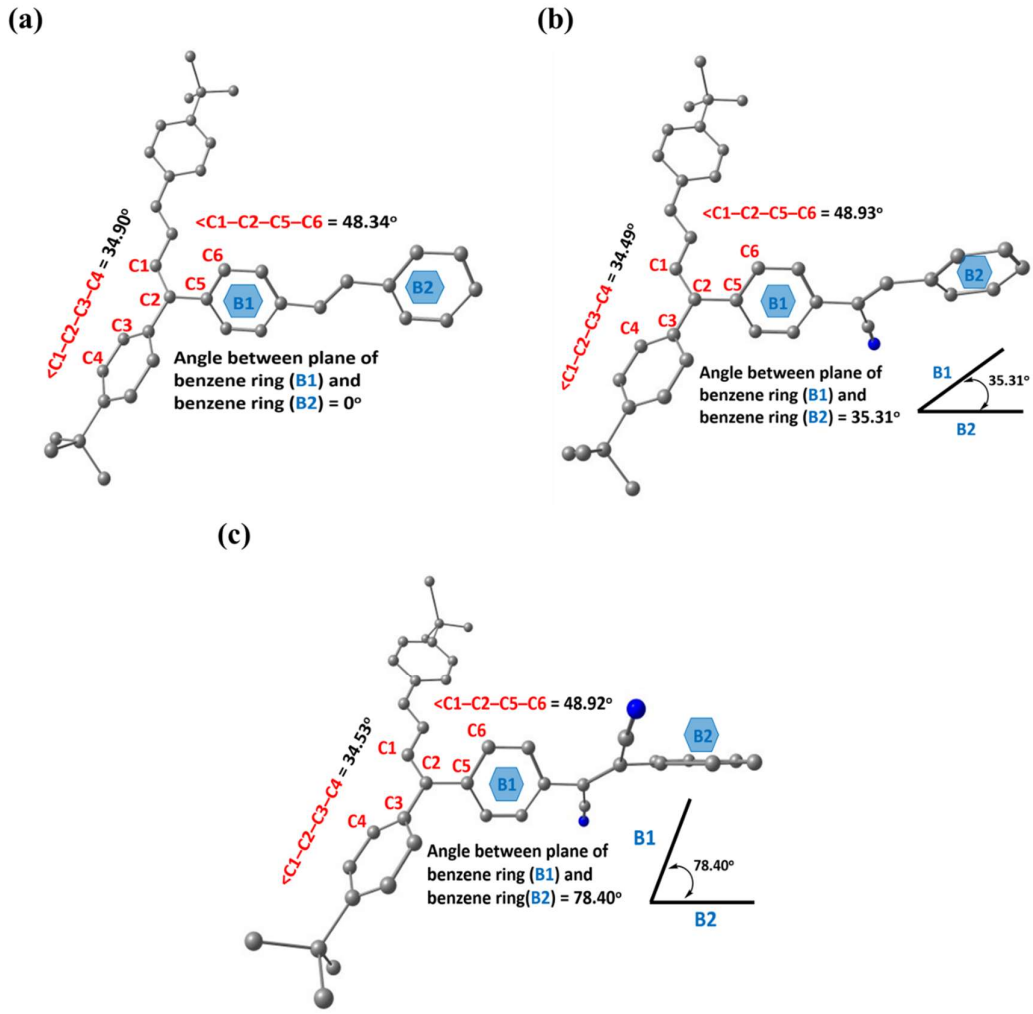

Fig. S32: Optimized geometry of repeating unit of copolymers (a) P1, (b) (P2) and (P3) showing the twisting angle between planes of two benzene unit of accepter part of the copolymers

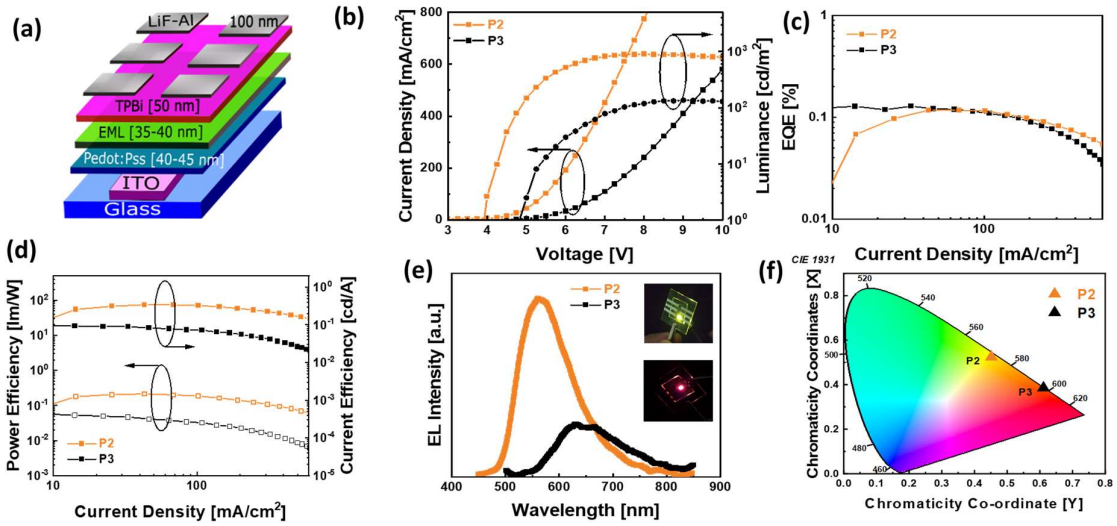

Fig. S33: Comparative device results of copolymers, P2 and P3 1(a) shows the device stack used same for P2 and P3 emitters. (b) J-V-L [current Density-Voltage-Luminance] curves. (c)The EQE and Current and (d) Power efficiency vs current density curves. (e) comparison of EL intensity of P2 and P3 (f) CIE color space of EL spectra of P2 and P3.

Table-S3: Comparative device results.

Polymer	**Turn On [V] 1 cd/m^2**	**Luminance [cd/m^2] @ 10/100/1000**	**EQE [%] @ 10/100/1000**	**CE[cd/A] @ 10/100/1000**	**PE [lm/W] @ 10/100/1000**	**CIE [X, Y]**
P2	3.9	10/337/891	0.02/0.11/0.03	0.15/0.32/0.15	0.11/0.19/0.03	[0.45,0.51]
P3	4.8	8/81/-	0.12/0.09/-	0.09/0.07/-	0.05/0.032/-	[0.47,0.27]

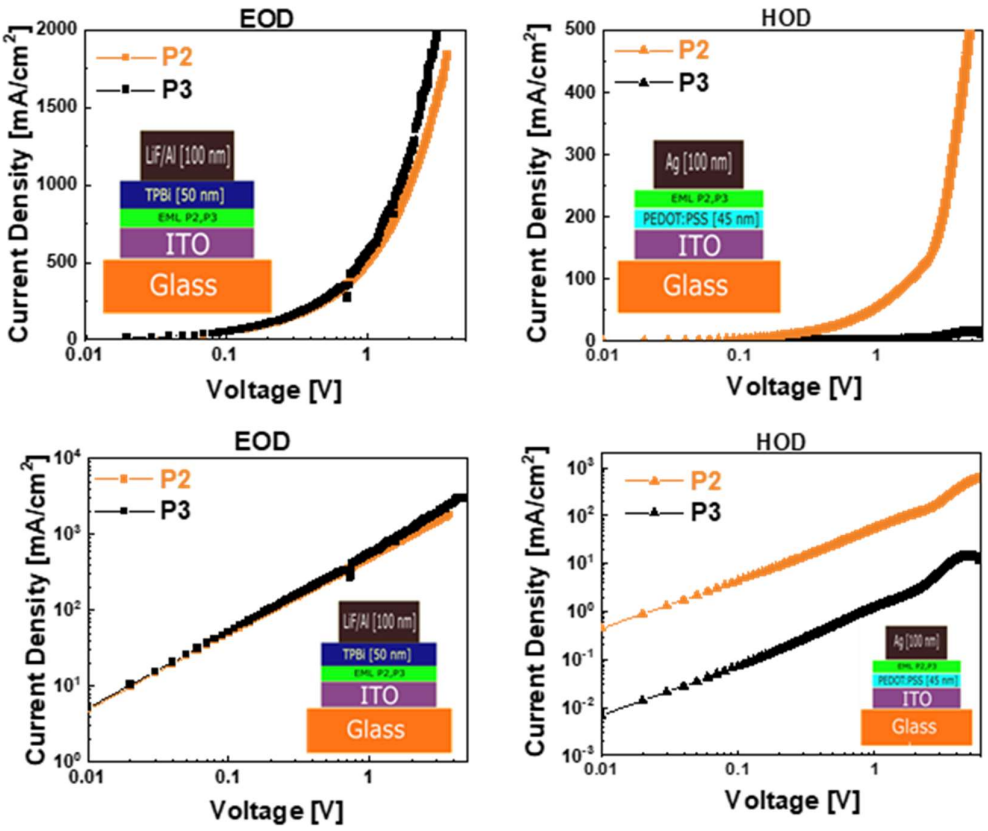

Fig. S34: Comparative I-V characteristics of single carrier transport devices for copolymers (P2 and P3). Electron-only device (EOD) and hole-only device (HOD) made from two copolymers P2 and P3 are showing more or less similar electron mobility and higher hole mobility of copolymer P2 than that of copolymer P3.

Table-S4: Solution processed **non-doped PLED** device results.

Polymer	Device Configuration	Device Result	Reference
Aryl-substituted buta-1,3-diene based (**P2**)	(ITO)/PEDOT: PSS (40-45 nm)/ **Polymer, P2** (35-40 nm)/TPBi(50 nm)/ LiF(1 nm)/ Al(100 nm)	$V_{turn-on}$ (V): 3.9; L_{max} (cd/m²): 903; CE_{max} (cd/A): 0.34; PE_{max} (lm/W): 0.21; EQE (%): 0.117	**Our work**
Aryl-substituted buta-1,3-diene copolymers (**P1, P2** and **P3**) with fluorene or carbazole	ITO/**polymer** (35 nm)/TPBI (40 nm)/LiF/Al	**P1**: λ_{ELmax} (λ_{PLmax}) 496 (491) nm; $V_{turn-on}$ 12.5 V; J_{max} 109 mA/cm²; L_{max} 144 cd/m²; η_{max} 0.19 cd/A; EQE 0.09 % **P3**: 512 (509) nm; 8.9 V; 242 mA/cm²; 520 cd/m²; 0.27 cd/A; 0.07 % **P5**: 528, 596 (525) nm; 11.5 V; 200 mA/cm²; 324 cd/m²; 0.20 cd/A; 0.08 %	**S2**
TPE based polymers (**P1**, **P2**, **P3** and **P4**)	ITO/PEDOT:PSS (25 nm)/Poly-TPD (25 nm)/**EML** (32 nm)/TPBI (35 nm)/Cs2CO3 (8 nm):Ag (100 nm)	**P1**: λ_{EL} 494 nm; V_{on} 8.7 V; Lumin (L) 574 (16.8) cd/m²; CD (J) 376 mA/cm²; CE 0.20 cd/A **P2**: 515 nm; 6.9 V; 1761 (15.0) cd/m²; 380 mA/cm²; 0.82 cd/A **P3**: 501 nm; 5.7 V; 3609 (12.9) cd/m²; 434 mA/cm²; 1.17 cd/A **P4**: 509 nm; 4.8 V; 3109 (12.6) cd/m²; 399 mA/cm²; 1.14 cd/A	**S3**
TPE based linear and hyperbranched polymers (**HP-TPE-Cz** and **LP-TPE-Cz**)	(ITO/PEDOT:PSS (25 nm)/Poly-TPD (25 nm)/**HP-TPE-Cz** or **LP-TPE-Cz** (32 nm)/TPBI (35 nm)/Cs2CO3 (8 nm):Ag (100 nm)	**HP-TPE-Cz**: λ_{EL} 508 nm; $V_{turn-on}$ 5.2 V; CE_{max} 2.13 cd/A; L_{max} 5914(14.4) cd/m²; CD 448 mA/cm; EQE 0.09 % **LP-TPE-Cz**: 500 nm; 8.0 V; 1.04 cd/A; 1654(16.2) cd/m²; 393 mA/cm; 0.07 %	**S4**
TPE based organic-inorganic hydride hyper-Branched polymer (**PFTPE-Ir(piq)$_3$-X**)	ITO/PEDOT:PSS (40 nm)/PFBT-Ir(piq)$_3$ (80 nm)/TPBi (40 nm)/LiF (1 nm)/Al (100 nm)	**WOLED-1**: PFTPE-Ir(piq)$_3$-1; Emission layer 492/632 nm; $Luminane_{max}$ **4067** cd/m²; CE_{max} 2.24 cd/A; EQE_{max} 0.91 %; CRI 71; CIE(x, y) (0.25, 0.36) **WOLED-2**: PFTPE-Ir(piq)$_3$-5; 496/636 nm; **4686** cd/m²; 2.43 cd/A; 1.08 %; 86; (0.26, 0.36) **WOLED-3**: PFTPE-Ir(piq)$_3$-10; 492/640 nm; **2277** cd/m²; 1.76 cd/A; 1.05 %; 71; (0.33, 0.34)	**S5**

Reference:
S1. M. Nakamura, M. Gon, K. Tanaka and Y. Chujo, *Macromolecules* 2023, **56**, 2709–2718.
S2. Y. Liu, X. Chen, J. Qin, G. Yu and Y. Liu, *Polymer*, 2010, **51**, 3730-3735.
S3. W. Wu, S. Ye, R. Tang, L. Huang, Q. Li, G. Yu, Y. Liu, J. Qin and Z. Li, *Polymer*, 2012, **53**, 3163-3171.
S4. W. Wu, S. Ye, L. Huang, L. Xiao, Y. Fu, Q. Huang, G. Yu, Y. Liu, J. Qin, Q. Lia and Z. Li, *J. Mater. Chem.*, 2012, **22**, 6374-6382.
S5. D. Wu, T. Zhang, J. Sun, Y. Wu, X. Liao, G. Lu, J. Yang, H. Wang, L. Li and B. Xu, *Tetrahedron*, 2018, **74**, 7218-7227.